

# Docking and Migration of Carbon Monoxide in Nitrogenase: The Case for Gated Pockets from Infrared Spectroscopy and Molecular Dynamics

Leland B. Gee,<sup>†</sup> Igor Leontyev,<sup>§</sup> Alexei Stuchebrukhov,<sup>†</sup> Aubrey D. Scott,<sup>†</sup> Vladimir Pelmenschikov,<sup>||</sup> and Stephen P. Cramer<sup>\*,†,‡,§</sup>

<sup>†</sup>Department of Chemistry, University of California, Davis, California 95616, United States

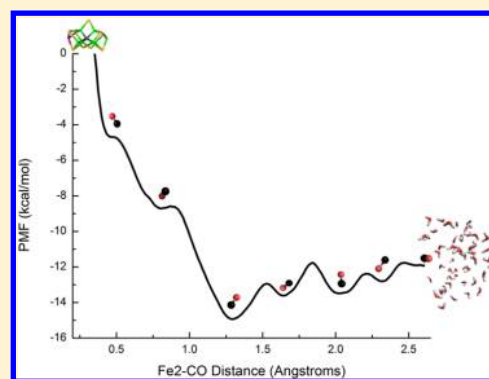
<sup>‡</sup>Physical Biosciences Division, Lawrence Berkeley National Laboratory, Berkeley, California 94720, United States

<sup>§</sup>InterX Inc., Berkeley, California 94710, United States

<sup>||</sup>Institut für Chemie, Technische Universität Berlin, 10623 Berlin, Germany

## S Supporting Information

**ABSTRACT:** Evidence of a CO docking site near the FeMo cofactor in nitrogenase has been obtained by Fourier transform infrared spectroscopy-monitored low-temperature photolysis. We investigated the possible migration paths for CO from this docking site using molecular dynamics calculations. The simulations support the notion of a gas channel with multiple internal pockets from the active site to the protein exterior. Travel between pockets is gated by the motion of protein residues. Implications for the mechanism of nitrogenase reactions with CO and N<sub>2</sub> are discussed.



Nitrogenase (N<sub>2</sub>ase) is the enzyme responsible for biological nitrogen fixation.<sup>1–3</sup> For molybdenum-containing N<sub>2</sub>ase from *Azotobacter vinelandii*, on which this work will focus, X-ray diffraction has revealed a unique [Mo-7Fe-9S-C]-homocitrate cluster at the active site of the MoFe protein of N<sub>2</sub>ase,<sup>4,5</sup> with an interstitial carbide at the center of a prismatic six-Fe cage.<sup>5–7</sup> This cluster, known as the FeMo cofactor (FeMo-co), is capable of reducing a wide variety of triply bonded substrates, such as N<sub>2</sub>, C<sub>2</sub>H<sub>2</sub>, HCN, and protons.<sup>8</sup> It has recently been shown that this enzyme can also produce C<sub>x</sub>H<sub>y</sub> hydrocarbons from CO<sup>9–11</sup> and even CH<sub>4</sub> from CO<sub>2</sub>.<sup>12,13</sup> The migration of substrates, such as N<sub>2</sub> and CO and protons, to the active site, as well as the exit of products such as NH<sub>3</sub>, various hydrocarbons C<sub>x</sub>H<sub>y</sub>, and H<sub>2</sub>, is clearly a critical part of N<sub>2</sub>ase reactivity.

Several different channels have been proposed for access to or from the FeMo cofactor.<sup>14–21</sup> In 2003, Igarashi and Seefeldt pointed out a candidate substrate channel starting near surface residues  $\alpha$ -K209 and  $\alpha$ -W205. This mostly hydrophobic pathway (now called the “IS channel”<sup>20</sup>) ultimately passes the  $\alpha$ -V70,  $\alpha$ -H195, and  $\alpha$ -R96 region and terminates at the Fe<sub>2,3,6,7</sub> face of the FeMo cofactor.<sup>14</sup> At the opposite end of the FeMo cofactor, a hydrophilic channel extends from a “water pool”<sup>15</sup> proximal to the homocitrate ligand, through the interface between subunits  $\alpha$  and  $\beta$ , and finally to the surface. Durrant offered this “interstitial channel” as an efficient path for

diffusion of both dinitrogen and ammonia,<sup>16</sup> and his proposition was later tested through site-directed mutagenesis work by Barney and co-workers.<sup>17</sup> Dance has noted a similar channel for the egress of ammonia, starting at  $\alpha$ -Q191.<sup>18</sup> Smith and co-workers have recently proposed a very different dynamic channel that opens and closes on a time scale of tens of nanoseconds, starting near surface residues  $\alpha$ -R281 and  $\alpha$ -H383 and leading to the Fe<sub>2,3,6,7</sub> face,<sup>19</sup> which may have a role in proton transport.<sup>22,23</sup> Additional substrate/product pathways have most recently been proposed by Morrison and co-workers, based on Caver calculations combined with analysis of binding sites for Xe and small molecules.<sup>20</sup> Apart from these small molecule channels, multiple proton relay chains (“proton bays” and “proton wires”), leading to S2B, S3B, and SSA were noted by Durrant<sup>16</sup> and more recently analyzed by Dance.<sup>21</sup>

Pockets and channels for small molecules like CO and O<sub>2</sub> have proven to be important in the study of myoglobin (Mb) dynamics,<sup>24</sup> and they have also been found to be important for hydrogenases,<sup>25</sup> cytochrome oxidase,<sup>26</sup> carbon monoxide dehydrogenase/acetyl-CoA synthase,<sup>27</sup> and many other “gas-processing” enzymes.<sup>28</sup> There is a flourishing literature about how to deduce and evaluate these conduits by computational

Received: February 28, 2015

Revised: April 26, 2015

Published: April 28, 2015

methods.<sup>29–34</sup> On the experimental side, the migration of CO following MbCO photolysis has been followed by infrared spectroscopy, including static,<sup>35</sup> picosecond time-resolved,<sup>36</sup> and temperature derivative<sup>37</sup> methods. Two photolysis product IR bands at 2131 and 2119  $\text{cm}^{-1}$ , labeled B<sub>1</sub> and B<sub>2</sub>, respectively, are observed for wild-type MbCO.<sup>35</sup> These have been taken as evidence of two different CO orientations at the Mb “docking site”,<sup>38</sup> and the magnitude of the splitting has allowed calculation of the interior electric field.<sup>37</sup> Extensive time-resolved X-ray diffraction studies have allowed observation of CO migration between different pockets within Mb<sup>39</sup> and the correlation of CO pockets with those observed under high-pressure Xe.<sup>40</sup>

Pockets and channels should certainly be relevant for understanding N<sub>2</sub>ase. Analogous to Mb, Xe pockets have been identified by X-ray crystallography in *Klebsiella pneumoniae*<sup>41</sup> and *Azotobacter vinelandii* (*Av*).<sup>42</sup> Recently, a detailed comparison of Xe sites in *Av* and *Clostridium pasteurianum* has been made, along with binding sites for CO and other small molecules.<sup>43</sup> In this paper, we present FT-IR cryophotolysis data that support a docking site for CO near the FeMo cofactor. We then use molecular dynamics calculations to identify a location for the docking site in *Av* Mo N<sub>2</sub>ase as well as a channel allowing for escape of CO and entry of N<sub>2</sub>.

## EXPERIMENTAL PROCEDURES

**Photolysis of CO-Nitrogenase.** The N<sub>2</sub>ase enzyme was prepared from *Av* and reacted with CO using the same protocol from our previous studies.<sup>23,44</sup> The infrared spectra were recorded with a Bruker Vertex 70v FT-IR instrument at cryogenic temperatures. Photolysis was induced by a broadband Sutter Instruments xenon-arc lamp. Samples were held in custom-built cells with Teflon spacers to give a path length of 70  $\mu\text{m}$ .

**Molecular Dynamics.** Simulations were performed using a customized force field in the Gromacs molecular dynamics package.<sup>45</sup> The MoFe N<sub>2</sub>ase-CO  $\alpha$  subunit was first energy minimized and then followed by dynamics at multiple temperatures.

More detailed information about all experimental methods is available in the Supporting Information.

## RESULTS

**Infrared Spectroscopy.** As shown in Figure 1, positive product bands appear upon low-temperature photolysis of CO-inhibited wild-type N<sub>2</sub>ase as well as the  $\alpha$ -H195Q variant. The 37  $\text{cm}^{-1}$  downshifts with <sup>13</sup>CO substitution confirm that these are indeed CO bands. By analogy with the MbCO literature, the absorption bands at 2135 and 2123  $\text{cm}^{-1}$  are consistent with “free CO” species adopting two orientations at a docking site.<sup>38</sup> We label the N<sub>2</sub>ase free CO bands NB<sub>1</sub> and NB<sub>2</sub>, respectively, by analogy to the myoglobin (Mb) CO labels.<sup>35</sup> For Mb mutants, additional bands have been observed to range from 2108 to 2152  $\text{cm}^{-1}$ , and we cannot rule out the existence of such minor species in N<sub>2</sub>ase.

There are differences between wild-type and  $\alpha$ -H195Q spectra that suggest that altering the amino acid environment around the FeMo cofactor has an effect on the photolyzed CO. In the wild-type enzyme, the NB<sub>2</sub> band at 2123  $\text{cm}^{-1}$  is more intense than the NB<sub>1</sub> band at 2135  $\text{cm}^{-1}$ . In  $\alpha$ -H195Q, the intensity pattern is reversed, and the asymmetry favors the NB<sub>1</sub> band, suggestive of two or more unresolved subspecies. Because

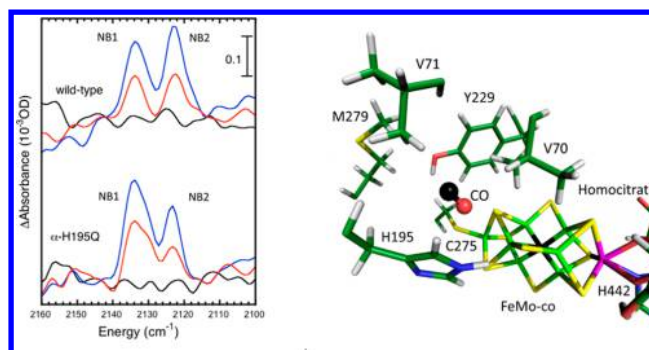


**Figure 1.** “Free CO” IR bands (left) in wild-type N<sub>2</sub>ase<sup>44</sup> vs H195Q N<sub>2</sub>ase. Curves represent photolysis difference (subtracting with a no photolysis background) spectra: baseline noise before photolysis (black), halfway through photolysis (red), and end point of photolysis (blue). Model (right) for CO in the docking site in one of the two orientations that could give rise to the observed splitting.

a small change in the side chain at position 195 affects the photolysis spectra, these results are at least consistent with locating the “free CO” close to that position.

**Molecular Dynamics.** Inspired by the experimental evidence of a CO docking site in N<sub>2</sub>ase, we began a molecular dynamics study of CO migration from that site, analogous to those used for myoglobin and related proteins.<sup>15,46</sup> In this work, we took advantage of a force field for the FeMo cofactor that had been previously validated by comparison with results from nuclear resonance vibrational spectroscopy (NRVS), as well as structural models for binding of CO to the FeMo cofactor from DFT calculations that have been tested against NRVS and EXAFS data.<sup>23</sup> We chose to initially place the CO near Fe2. Our previous work has shown the photolabile “Hi-1” CO form has a terminal CO and a formyl-like species.<sup>47</sup> Likewise, Fe6 has been implicated as the most reactive site on the FeMo cofactor;<sup>48</sup> therefore, we presume Fe6 binds the more reduced formyl-like species and Fe2 binds the terminal CO species that photolyzes to free CO. The entire protein structure was then relaxed to minimize any forces resulting from CO insertion. This yielded an initial Fe2–CO distance of 4.2 Å. The CO was then allowed to migrate through the protein at various temperatures, including 10, 80, 150, 200, 250, and 300 K. The motion of the CO and the protein was followed out to 10 ns (Figure 2).

The molecular dynamics calculations find a candidate “docking site” with the CO ~5 Å from Fe2 (Figure 1, right, and Figure 2). In this location, CO is within H-bonding distance of  $\alpha$ -His-195 N $\epsilon$  (3.1 Å). Another residue within H-bonding distance is  $\alpha$ -Y229 (O–O distance of 4.1 Å). Finally, the critical  $\alpha$ -V70 side chain is in position to constrain the CO motion. This bears some resemblance to the docking site in myoglobin, where photolyzed CO is within H-bonding distance of H64 and is further trapped by aliphatic side chains of L29 and I107 after photolysis.<sup>38,39,49</sup> As illustrated by the time courses plotted for different temperatures (Figure 3), at 10 K the CO remains in the docking site, but at higher temperatures, it rapidly migrates to three distinct regions that are progressively larger distances from the FeMo cofactor.

Upon departure from the docking site, the overall motion was stochastic and bidirectional. However, the path that was most frequently taken was strikingly similar to the IS channel.<sup>14</sup> Our result is compared with other proposed channels and pockets in Figure 3. The channel begins near key residues  $\alpha$ -

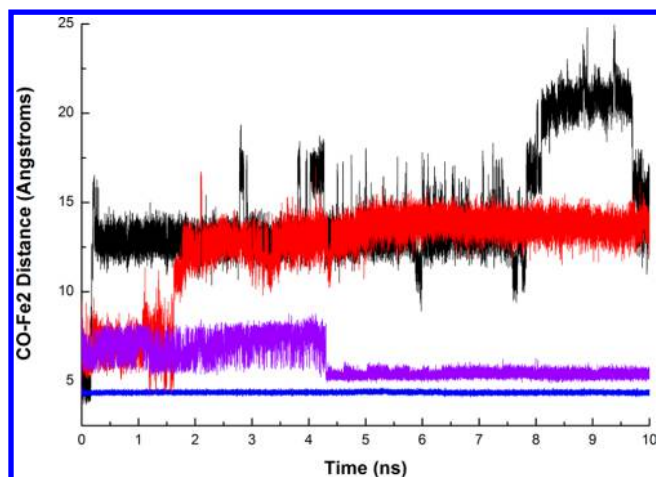


**Figure 2.** Typical time-dependent traces for CO migration at different temperatures [300 K (black), 250 K (red), 150 K (purple), and 10 K (blue)].

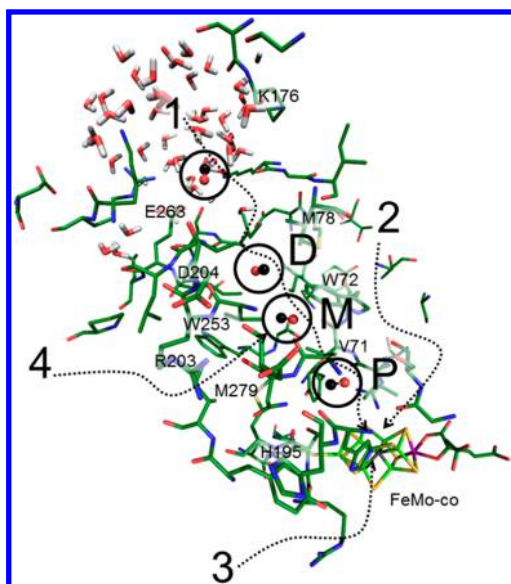


**Figure 3.** Some of the many pathways that have been proposed: (1) Igarashi and Seefeldt,<sup>14</sup> (2) Barney,<sup>17</sup> (3) Smith,<sup>19</sup> and (4) Morrison.<sup>20</sup> Also, the following pockets were observed in this work: P, proximal; M, medial; and D, distal. Residue labels are given to provide a frame of reference and outline the channel path. The CO in the dynamics calculations follows the channel predicted by Igarashi (labeled 1 in the figure).

H195 and  $\alpha$ -V70, and it ends near surface residues  $\alpha$ -M78,  $\alpha$ -V179, and  $\alpha$ -V206 and  $\alpha$ -I259 (Figure 3). Although this might seem to be only a confirmation of the Igarashi channel, from the dynamics calculation we see that the migration of CO is not uniform over time (Figure 3). Rather, just as in myoglobin and other proteins,<sup>50</sup> the CO was relatively stable in several distinct sites, the initial “docking site” and three distinct “pockets”. Passage from the docking site and between pockets is governed by occasional gate openings by key residues along the channel through thermodynamic fluctuations. We now discuss the sites where the CO spent most of the time.

The first pocket encountered (after leaving the docking site) has the CO center of mass (COM) 9.5 Å from the FeMo cofactor central carbide, with a closest approach to Fe2 of 8.5 Å (Figure 4a). Key side chains in this pocket include  $\alpha$ -M279,  $\alpha$ -

V71, and  $\alpha$ -S278. Unlike the later pockets, this first pocket also includes a tyrosine side chain,  $\alpha$ -Y229, a good candidate for hydrogen bonding to CO. As the closest pocket to the docking site, we label this the proximal or P-pocket.

The second (“medial” or “M”) pocket seen in the MD simulations contains  $\alpha$ -W253,  $\alpha$ -S254, and  $\alpha$ -I282 (Figure 4b). It is gated from the previous pocket by  $\alpha$ -N199,  $\alpha$ -M279,  $\alpha$ -V71, and  $\alpha$ -A198. The four residues sterically prevent CO from returning to the previous pocket, but they can open during thermal fluctuations. When CO is trapped within the M-pocket, the Fe2–CO distance is  $\sim$ 13.0 Å. We gain confidence in this predicted location for CO because it coincides with the Xe1 pocket seen by X-ray diffraction.<sup>20</sup> As shown in Figure 4b, our typical CO position overlaps nicely with the Xe position observed by Rees and co-workers.<sup>20,42</sup>

The third (“distal” or “D”) pocket observed in our calculations involves  $\alpha$ -I259,  $\alpha$ -V206,  $\alpha$ -M78, and  $\alpha$ -V179 (Figure 4c). Access to the D-pocket from the M-pocket is gated by residues  $\alpha$ -V202,  $\alpha$ -I75, and  $\alpha$ -W72. All of the aforementioned side chains are part of the IS channel proposed by Igarashi and Seefeldt.<sup>14</sup> The average Fe2–CO distance from within the D-pocket was 17 Å. We note that a final region for CO occupation was located beyond the D-pocket and within a solvent interaction crater on the surface of the protein. This region had an average Fe2–CO distance of  $\sim$ 21 Å. Penetration into the solvent occurred at a distance of  $\sim$ 25 Å.

Because  $N_2$  is the natural substrate for  $N_2$ ase, we also performed a simulation at 300 K using  $N_2$  as the diatomic in motion. As expected,  $N_2$  behaved like CO and bidirectionally traversed through the three pockets and into the solvent space (Figure S1 of the Supporting Information). In this simulation, the  $N_2$  spent most of its time in the M-pocket, just as we observed with CO.

**An Energy Surface.** The motion of CO within  $N_2$ ase appears to involve capture within pockets interlaced with occasional gate openings. We decided to map the potential energy surface for this motion of CO within the protein by performing a potential of mean force (PMF) calculation using GROMACS.<sup>51</sup> This involved sampling multiple Fe2–CO distances and forcing them to evolve individually over time. The results from these calculations are shown in Figure 4d. The first minimum is a shallow well at 5 Å that corresponds to the proposed docking site. At longer distances, there are three distinct potential minima corresponding to each identified pocket in the channel. Beyond these wells, we see the solvent interaction crater at 20 Å and solvent space at  $\sim$ 25 Å. An important result from these calculations is that the location identified as the medial pocket is the lowest-energy location where CO can reside.

The overall scale of the PMF is similar to what is seen in previous work for a ligand in the different channel proposed recently;<sup>19</sup> however, the PMF defined in this work has potential wells with depths greater than what is seen for that channel. The M-pocket has the largest barriers in both direction: 1.9 kcal/mol toward the D-pocket and 7.4 kcal/mol for CO moving toward the P-pocket.

## DISCUSSION

Our calculations are the first use of molecular dynamics to include an experimentally constrained force field for the FeMo cofactor. By combining these calculations with IR-monitored cryogenic photolysis, we have found the first evidence of a CO docking site in  $N_2$ ase. We favor this docking site as the most

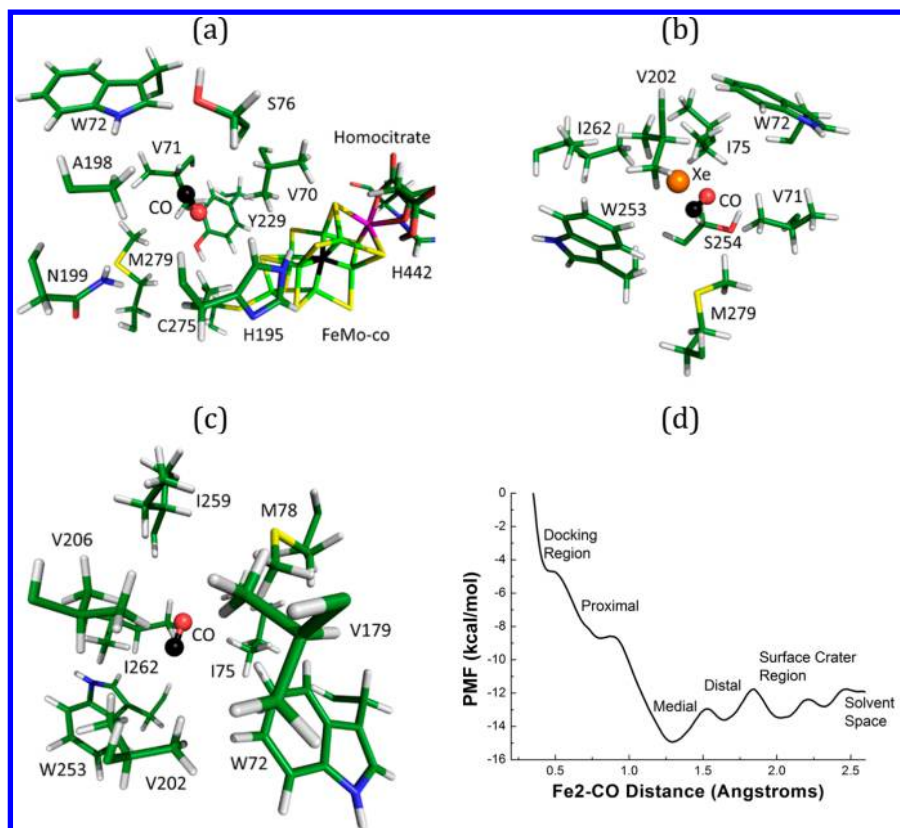


**Figure 4.** (a) Illustration of the proximal pocket, (b) medial pocket with xenon overlaid from Morrison et al.,<sup>20</sup> (c) distal pocket, and (d) profile of the interaction energy between CO and the system vs the Fe2–CO distance along the proposed channel from the FeMo cofactor to the solvent space.

likely position for free CO following cryogenic photolysis. The docking site is adjacent to the FeMo cofactor and has two possible hydrogen bonding partners for CO,  $\alpha$ -H195 and  $\alpha$ -Y229. In myoglobin, H-bonding to H64 is considered to be important for the 12  $\text{cm}^{-1}$  splitting of product bands B<sub>1</sub> and B<sub>2</sub> at 2131 and 2119  $\text{cm}^{-1}$ , respectively. Substitution of histidine with leucine in the H64L variant in myoglobin causes the loss of that splitting and yields a single product band at 2126  $\text{cm}^{-1}$ .<sup>38</sup> H-Bonding to  $\alpha$ -H195 or  $\alpha$ -Y229 may play a similar role in splitting the “free CO” bands of photolyzed N<sub>2</sub>ase.

Using the MD calculations, by following the path of CO or N<sub>2</sub> starting near this docking site, we discovered a channel for these molecules from the FeMo cofactor to the protein exterior, in a location consistent with a previous proposal from static CAVER calculations.<sup>14</sup> A benefit from the dynamics simulations is that they reveal a novel gating mechanism for migration of CO or N<sub>2</sub> through this hydrophobic channel, a feature that cannot be observed from static calculations. We find that CO spends most of its time in distinct pockets, and travel between pockets is allowed by gating motions of neighboring amino acids.

Although the exact mechanism of N<sub>2</sub>ase catalysis is far from understood, all proposed reaction pathways require multiple electron and proton transfers to the FeMo cofactor region before any ligand binding can occur. In particular, the popular Lowe–Thornley (LT) model for the N<sub>2</sub>ase reaction pathway<sup>52</sup> posits three or four electron/proton transfers to the FeMo cofactor and/or its associated ligands before N<sub>2</sub> binding. In the absence of substrate binding, the LT model proposes that the FeMo cofactor will oxidize through H<sub>2</sub> evolution.<sup>8</sup>

It has been argued that because N<sub>2</sub>ase is a slow enzyme, it has no need for a hydrophobic tunnel that would allow rapid gas access to the FeMo cofactor.<sup>28</sup> However, the pockets and gates that we observe may play a role in optimizing N<sub>2</sub>ase catalytic efficiency. By trapping an N<sub>2</sub> molecule in the M-pocket, the enzyme would have substrate available for binding within a few nanoseconds of reaching the E<sub>3</sub> or E<sub>4</sub> level. This might help minimize “futile” H<sub>2</sub> production that might occur if N<sub>2</sub> were not immediately available. These gated “storage” pockets would allow for N<sub>2</sub> availability whenever the FeMo cofactor reaches the appropriate level of reduction. In a similar vein, it has been proposed that large sections of tunnels serve as H<sub>2</sub> “gas reservoirs” in hydrogenases.<sup>53,54</sup>

Weyman and co-workers studied the  $\alpha$ -V75I and  $\alpha$ -V76I variants in a similar N<sub>2</sub>ase from *Anabaena variabilis* (which would correspond to  $\alpha$ -V70I and  $\alpha$ -V71I in *Av*),<sup>55</sup> although as expected, their  $\alpha$ -V75I variant showed reduced N<sub>2</sub> fixation activity and the  $\alpha$ -V76I substitution had no effect. Because our proposal for gated access between pockets is dynamic, we can accommodate these findings by simply allowing for comparable gating by isoleucine or valine residues at *Av* position 71.

Some of the other channels illustrated in Figure 3 presumably play a role in the egress of the mandatory H<sub>2</sub> coproduct as well as NH<sub>3</sub> or NH<sub>4</sub><sup>+</sup>. In this area, we are agnostic, because Lautier has noted that hydrophobic molecules sometimes travel through hydrophilic channels and vice versa.<sup>56</sup> However, it seems unlikely that evolved H<sub>2</sub> would exit through our proposed substrate channel, because this might limit the influx of N<sub>2</sub> to the FeMo cofactor. It seems logical that N<sub>2</sub>ase would have a mechanism or “pressure relief” for the

active site region to release H<sub>2</sub> from the active site without interfering with the catalytic process. Overall, N<sub>2</sub>ase has to handle the flow of electrons, protons, N<sub>2</sub>, H<sub>2</sub>, and NH<sub>3</sub>, and the nature of “traffic control” in this remarkable enzyme remains incompletely understood.

## ■ ASSOCIATED CONTENT

### ■ Supporting Information

A detailed description of the methods and dynamics course for N<sub>2</sub> and an image of the crater region (Figures S1 and S2, respectively). The Supporting Information is available free of charge on the ACS Publications website at DOI: 10.1021/acs.biochem.5b00216.

## ■ AUTHOR INFORMATION

### Corresponding Author

\*E-mail: spjcramer@ucdavis.edu.

### Funding

This work was funded by National Institutes of Health Grant GM-65440, and the National Science Foundation grant CHE 1308384 (S.P.C.). The work by V.P. was supported by the “Unifying Concepts in Catalysis” (UniCat) cluster of excellence.

### Notes

The authors declare no competing financial interest.

## ■ ACKNOWLEDGMENTS

Computational work was performed on the Hopper Supercomputing Cluster from the National Energy Research Scientific Computing center through ERCAP Request 87354. We thank William Newton and Christie Dapper for scientific discussions and assistance with the manuscript.

## ■ ABBREVIATIONS

*Av*, *A. vinelandii*; N<sub>2</sub>, dinitrogen; CO, carbon monoxide; N<sub>2</sub>ase, nitrogenase; FeMo-co, iron–molybdenum cofactor of the MoFe protein; MoFe protein, larger molybdenum–iron-containing protein of nitrogenase; Fe protein, smaller iron-containing protein of nitrogenase; IR, infrared; FT-IR, Fourier transform infrared spectroscopy; MB, myoglobin; MBCO, myoglobin inhibited with CO; PMF, potential of mean force; LT, Lowe–Thorneley model of nitrogen fixation; NRVS, nuclear resonant vibrational spectroscopy; EXAFS, extended x-ray absorbance fine structure; DFT, density functional theory.

## ■ REFERENCES

- (1) Hoffman, B. M., Dean, D. R., and Seefeldt, L. C. (2009) Climbing Nitrogenase: Toward a Mechanism of Enzymatic Nitrogen Fixation. *Acc. Chem. Res.* 42, 609–619.
- (2) Seefeldt, L. C., Hoffman, B. M., and Dean, D. R. (2009) Mechanism of Mo-Dependent Nitrogenase. *Annu. Rev. Biochem.* 78, 701–722.
- (3) Canfield, D. E., Glazer, A. N., and Falkowski, P. G. (2010) The Evolution and Future of Earth’s Nitrogen Cycle. *Science* 330, 192–196.
- (4) Einsle, O., Tezcan, F. A., Andrade, S. L. A., Schmid, B., Yoshida, M., Howard, J. B., and Rees, D. C. (2002) Nitrogenase MoFe-Protein at 1.16 Å Resolution: A Central Ligand in the FeMo-Cofactor. *Science* 297, 1696–1700.
- (5) Spatzal, T., Aksoyoglu, M., Zhang, L., Andrade, S. L. A., Schleicher, E., Weber, S., Rees, D. C., and Einsle, O. (2011) Evidence for Interstitial Carbon in Nitrogenase FeMo Cofactor. *Science* 334, 940.

- (6) Lancaster, K. M., Roemelt, M., Ettenhuber, P., Hu, Y. L., Ribbe, M. W., Neese, F., Bergmann, U., and DeBeer, S. (2011) X-ray Emission Spectroscopy Evidences a Central Carbon in the Nitrogenase Iron-Molybdenum Cofactor. *Science* 334, 974–977.

- (7) Wiig, J. A., Hu, Y., Lee, C. C., and Ribbe, M. W. (2012) Radical SAM-Dependent Carbon Insertion into the Nitrogenase M-Cluster. *Science* 337, 1672–1675.

- (8) Burgess, B. K., and Lowe, D. J. (1996) Mechanism of molybdenum nitrogenase. *Chem. Rev.* 96, 2983–3011.

- (9) Lee, C. C., Hu, Y., and Ribbe, M. W. (2010) Vanadium Nitrogenase Reduces CO. *Science* 329, 642.

- (10) Lee, C. C., Hu, Y. L., and Ribbe, M. W. (2011) Tracing the Hydrogen Source of Hydrocarbons Formed by Vanadium Nitrogenase. *Angew. Chem.* 50, 5545–5547.

- (11) Yang, Z.-Y., Dean, D. R., and Seefeldt, L. C. (2011) Molybdenum Nitrogenase Catalyzes the Reduction and Coupling of CO to Form Hydrocarbons. *J. Biol. Chem.* 286, 19417–19421.

- (12) Yang, Z.-Y., Moure, V. R., Dean, D. R., and Seefeldt, L. C. (2012) Carbon dioxide reduction to methane and coupling with acetylene to form propylene catalyzed by remodeled nitrogenase. *Proc. Natl. Acad. Sci. U.S.A.* 109, 19644–19648.

- (13) Seefeldt, L. C., Yang, Z.-Y., Duval, S., and Dean, D. R. (2013) Nitrogenase reduction of carbon-containing compounds. *Biochim. Biophys. Acta* 1827, 1102–1111.

- (14) Igarashi, R. Y., and Seefeldt, L. C. (2003) Nitrogen Fixation: The Mechanism of the Mo-Dependent Nitrogenase. *Crit. Rev. Biochem. Mol. Biol.* 38, 351–384.

- (15) Elber, R. (2010) Ligand diffusion in globins: Simulations versus experiment. *Curr. Opin. Struct. Biol.* 20, 162–167.

- (16) Durrant, M. C. (2001) Controlled protonation of iron-molybdenum cofactor by nitrogenase: A structural and theoretical analysis. *Biochem. J.* 355, 569–576.

- (17) Barney, B. M., Yurth, M. G., Dos Santos, P. C., Dean, D. R., and Seefeldt, L. C. (2009) A substrate channel in the nitrogenase MoFe protein. *JBIC, J. Biol. Inorg. Chem.* 14, 1015–1022.

- (18) Dance, I. (2013) A molecular pathway for the egress of ammonia produced by nitrogenase. *Sci. Rep.* 3, 1–9.

- (19) Smith, D., Danyal, K., Raugei, S., and Seefeldt, L. C. (2014) Substrate channel in nitrogenase revealed by a molecular dynamics approach. *Biochemistry* 53, 2278–2285.

- (20) Morrison, C. N., Hoy, J. A., Zhang, L., Einsle, O., and Rees, D. C. (2015) Substrate Pathways in the Nitrogenase MoFe Protein by Experimental Identification of Small Molecule Binding Sites. *Biochemistry* 54, 2052–2060.

- (21) Dance, I. (2012) The controlled relay of multiple protons required at the active site of nitrogenase. *Dalton Trans.* 41, 7647–7659.

- (22) Fisher, K., Hare, N. D., and Newton, W. E. (2014) Another role for CO with nitrogenase? CO stimulates hydrogen evolution catalyzed by variant *Azotobacter vinelandii* Mo-nitrogenases. *Biochemistry* 53, 6151–6160.

- (23) Scott, A., Pelmenschikov, V., Guo, Y., Wang, H., Yan, L., George, S., Dapper, C., Newton, W., Yoda, Y., Tanaka, Y., and Cramer, S. P. (2014) Structural Characterization of CO-Inhibited Mo-Nitrogenase by Combined Application of NRVS, EXAFS, and DFT: New Insights into the Effects of CO Binding and the Role of the Interstitial Atom. *J. Am. Chem. Soc.* 136, 15942–15954.

- (24) Meuwly, M. (2007) Using small molecules to probe protein cavities: The myoglobin–XO (X = C, N) family of systems. *The European Physical Journal Special Topics* 141, 209–216.

- (25) Hong, G. Y., and Pachter, R. (2012) Inhibition of Biocatalysis in Fe-Fe Hydrogenase by Oxygen: Molecular Dynamics and Density Functional Theory Calculations. *ACS Chem. Biol.* 7, 1268–1275.

- (26) Luna, V. M., Chen, Y., Fee, J. A., and Stout, C. D. (2008) Crystallographic studies of Xe and Kr binding within the large internal cavity of cytochrome *ba*<sub>3</sub> from *Thermus thermophilus*: Structural analysis and role of oxygen transport channels in the heme-Cu oxidases. *Biochemistry* 47, 4657–4665.

- (27) Doukov, T. I., Blasiak, L. C., Seravalli, J., Ragsdale, S. W., and Drennan, C. L. (2008) Xenon in and at the end of the tunnel of

bifunctional carbon monoxide dehydrogenase/acetyl-CoA synthase. *Biochemistry* 47, 3474–3483.

(28) Fontecilla-Camps, J. C., Amara, P., Cavazza, C., Nicolet, Y., and Volbeda, A. (2009) Structure-function relationships of anaerobic gas-processing metalloenzymes. *Nature* 460, 814–822.

(29) Petrek, M., Otyepka, M., Banas, P., Kosinova, P., Koca, J., and Damborsky, J. (2006) CAVER: A new tool to explore routes from protein clefts, pockets and cavities. *BMC Bioinf.* 7, 316.

(30) Yaffe, E., Fishelovitch, D., Wolfson, H. J., Halperin, D., and Nussinov, R. (2008) MolAxis: Efficient and accurate identification of channels in macromolecules. *Proteins: Struct., Funct., Bioinf.* 73, 72–86.

(31) Raunest, M., and Kandt, C. (2011) dxTuber: Detecting protein cavities, tunnels and clefts based on protein and solvent dynamics. *J. Mol. Graphics Modell.* 29, 895–905.

(32) Lin, T. L., and Song, G. (2011) Efficient mapping of ligand migration channel networks in dynamic proteins. *Proteins: Struct., Funct., Bioinf.* 79, 2475–2490.

(33) Schmidtke, P., Bidon-Chanal, A., Luque, F. J., and Barril, X. (2011) MDpocket: Open-source cavity detection and characterization on molecular dynamics trajectories. *Bioinformatics* 27, 3276–3285.

(34) Berka, K., Hanak, O., Sehnal, D., Banas, P., Navratilova, V., Jaiswal, D., Ionescu, C. M., Varekova, R. S., Koca, J., and Otyepka, M. (2012) MOLEonline 2.0: Interactive web-based analysis of biomacromolecular channels. *Nucleic Acids Res.* 40, W222–W227.

(35) Alben, J. O., Beece, D., Bowne, S. F., Doster, W., Eisenstein, L., Frauenfelder, H., Good, D., McDonald, J. D., Marden, M. C., Moh, P. P., Reinisch, L., Reynolds, A. H., Shyamsunder, E., and Yue, K. T. (1982) Infrared spectroscopy of photodissociated carboxymyoglobin at low temperatures. *Proc. Natl. Acad. Sci. U.S.A.* 79, 3744–3748.

(36) Lim, M. H., Jackson, T. A., and Anfinsen, P. A. (1995) Midinfrared Vibrational-Spectrum of CO after Photodissociation from Heme: Evidence for a Ligand Docking Site in the Heme Pocket of Hemoglobin and Myoglobin. *J. Chem. Phys.* 102, 4355–4366.

(37) Lehle, H., Kriegl, J. M., Nienhaus, K., Deng, P. C., Fengler, S., and Nienhaus, G. U. (2005) Probing electric fields in protein cavities by using the vibrational Stark effect of carbon monoxide. *Biophys. J.* 88, 1978–1990.

(38) Nienhaus, K., Olson, J. S., Franzen, S., and Nienhaus, G. U. (2005) The origin of stark splitting in the initial photoproduct state of MbCO. *J. Am. Chem. Soc.* 127, 40–41.

(39) Srajer, V., Ren, Z., Teng, T. Y., Schmidt, M., Ursby, T., Bourgeois, D., Pradervand, C., Schildkamp, W., Wulff, M., and Moffat, K. (2001) Protein conformational relaxation and ligand migration in myoglobin: A nanosecond to millisecond molecular movie from time-resolved Laue X-ray diffraction. *Biochemistry* 40, 13802–13815.

(40) Tetreau, C., Blouquit, Y., Novikov, E., Quiniou, E., and Lavalette, D. (2004) Competition with xenon elicits ligand migration and escape pathways in myoglobin. *Biophys. J.* 86, 435–447.

(41) Mayer, S. M. (2000) X-ray structure determination of *Klebsiella pneumoniae* nitrogenase component I. Ph.D. Thesis, University of East Anglia, Norfolk, U.K.

(42) Rees, D. C., Tezcan, F. A., Haynes, C. A., Walton, M. Y., Andrade, S., Einsle, O., and Howard, J. B. (2005) Structural basis of biological nitrogen fixation. *Philos. Trans. R. Soc., A* 363, 971–984.

(43) Daskalakis, V., and Varotsis, C. (2009) Binding and Docking Interactions of NO, CO and O<sub>2</sub> in Heme Proteins as Probed by Density Functional Theory. *Int. J. Mol. Sci.* 10, 4137–4156.

(44) Yan, L., Dapper, C. H., George, S. J., Wang, H.-X., Mitra, D., Dong, W.-B., Newton, W. E., and Cramer, S. P. (2011) Photolysis of 'Hi-CO' Nitrogenase: Observation of a Plethora of Distinct CO Species via Infrared Spectroscopy. *Eur. J. Inorg. Chem.* 2011, 2064–2074.

(45) Pronk, S., Páll, S., Schulz, R., Larsson, P., Bjelkmar, P., Apostolov, R., Shirts, M. R., Smith, J. C., Kasson, P. M., van der Spoel, D., Hess, B., and Lindahl, E. (2013) GROMACS 4.5: A high-throughput and highly parallel open source molecular simulation toolkit. *Bioinformatics* 29, 845–854.

(46) Elber, R., and Karplus, M. (1990) Enhanced Sampling in Molecular Dynamics: Use of the Time-Dependent Hartree Approx-

imation for a Simulation of Carbon-Monoxide Diffusion through Myoglobin. *J. Am. Chem. Soc.* 112, 9161–9175.

(47) Yan, L. F., Pelmenschikov, V., Dapper, C. H., Scott, A. D., Newton, W. E., and Cramer, S. P. (2012) IR-Monitored Photolysis of CO-Inhibited Nitrogenase: A Major EPR-Silent Species with Coupled Terminal CO Ligands. *Chem.—Eur. J.* 18, 16349–16357.

(48) Sarma, R., Barney, B. M., Keable, S., Dean, D. R., Seefeldt, L. C., and Peters, J. W. (2010) Insights into substrate binding at FeMoco-factor in nitrogenase from the structure of an  $\alpha$ -70(Ile) MoFe protein variant. *J. Inorg. Biochem.* 104, 385–389.

(49) Nutt, D. R., and Meuwly, M. (2003) Theoretical investigation of infrared spectra and pocket dynamics of photodissociated carbon-monoxo myoglobin. *Biophys. J.* 85, 3612–3623.

(50) Abbruzzetti, S., Spyraakis, F., Bidon-Chanal, A., Luque, F. J., and Viappiani, C. (2013) Ligand migration through hemoprotein cavities: Insights from laser flash photolysis and molecular dynamics simulations. *Phys. Chem. Chem. Phys.* 15, 10686–10701.

(51) Van der Spoel, D., Lindahl, E., Hess, B., Groenhof, G., Mark, A. E., and Berendsen, H. J. C. (2005) GROMACS: Fast, flexible, and free. *J. Comput. Chem.* 26, 1701–1718.

(52) Burgess, B. K., and Lowe, D. J. (1996) Mechanism of Molybdenum Nitrogenase. *Chem. Rev.* 96, 2983–3012.

(53) Chandrayan, S. K., McTernan, P. M., Hopkins, R. C., Sun, J. S., Jenney, F. E., and Adams, M. W. W. (2012) Engineering Hyperthermophilic Archaeon *Pyrococcus furiosus* to Overproduce Its Cytoplasmic [NiFe]-Hydrogenase. *J. Biol. Chem.* 287, 3257–3264.

(54) Montet, Y., Amara, P., Volbeda, A., Vernede, X., Hatchikian, E. C., Field, M. J., Frey, M., and Fontecilla-Camps, J. C. (1997) Gas access to the active site of Ni-Fe hydrogenases probed by X-ray crystallography and molecular dynamics. *Nat. Struct. Biol.* 4, 523–526.

(55) Weyman, P. D., Pratte, B., and Thiel, T. (2010) Hydrogen production in nitrogenase mutants in *Anabaena variabilis*. *FEMS Microbiol. Lett.* 304, 55–61.

(56) Lautier, T., Ezanno, P., Baffert, C., Fourmond, V., Cournac, L., Fontecilla-Camps, J. C., Soucaille, P., Bertrand, P., Meynial-Salles, I., and Leger, C. (2011) The quest for a functional substrate access tunnel in FeFe hydrogenase. *Faraday Discuss.* 148, 385–407.